NUWC-NPT Technical Report 12,163
30 September 2014

Characterization of the Boundary Layers on Full-Scale Bluefin Tuna

Kimberly M. Cipolla
Sensors and Sonar Systems Department

Naval Undersea Warfare Center Division
Newport, Rhode Island

PREFACE

This report was funded by the Naval Undersea Warfare Center Division Newport, under Section 219 Research Project, "Characterization of the Boundary Layers on Full-Scale Bluefin Tuna," principal investigator Kimberly M. Cipolla (Code 1512) and associate investigators Brian Amaral and Charles Henoch.

The technical reviewer for this report was Brian K. Amaral (Code 1522).

The author thanks Barbara Block (Stanford University), head of the Tuna Research and Conservation Center (TRCC) at the Hopkins Marine Station in Monterey, CA, for her collaborative spirit and discussions.

Reviewed and Approved: 30 September 2014

Ronald A. Vien
Head, Sensors and Sonar Systems Department

REPORT DOCUMENTATION PAGE

Form Approved
OMB No. 0704-0188

1. REPORT DATE (*DD-MM-YYYY*)	2. REPORT TYPE	3. DATES COVERED (*From – To*)
30-09-2014	Technical Report	

4. TITLE AND SUBTITLE

Characterization of the Boundary Layers on Full-Scale Bluefin Tuna

5a. CONTRACT NUMBER

5b. GRANT NUMBER

5c. PROGRAM ELEMENT NUMBER

6. AUTHOR(S)

Kimberly M. Cipolla

5.d PROJECT NUMBER

5e. TASK NUMBER

5f. WORK UNIT NUMBER

7. PERFORMING ORGANIZATION NAME(S) AND ADDRESS(ES)

Naval Undersea Warfare Center Division
1176 Howell Street
Newport, RI 02841-1708

8. PERFORMING ORGANIZATION REPORT NUMBER

TR 12,163

9. SPONSORING/MONITORING AGENCY NAME(S) AND ADDRESS(ES)

Naval Undersea Warfare Center Division
1176 Howell Street
Newport, RI 02841-1708

10. SPONSORING/MONITOR'S ACRONYM
NUWC

11. SPONSORING/MONITORING REPORT NUMBER

12. DISTRIBUTION/AVAILABILITY STATEMENT

Approved for public release; distribution is unlimited.

13. SUPPLEMENTARY NOTES

14. ABSTRACT

The physics that enable tuna to cross large expanses of ocean while feeding and avoiding predators is not understood; it is widely held that complex control of turbulent boundary layer transition and drag reduction are involved. Although the typical swimming speeds of bluefin tuna are 1 – 2 m/s, they can be higher during strong accelerations. The goal of the work documented in this report was to experimentally determine the approximate lateral location at which transition to turbulence occurs on the tuna for various speeds. The question is whether laminar flow or an advanced propulsion mechanism (or both) allows them to swim at high speeds. A full-scale model of a Pacific bluefin tuna was fabricated using a mold made from an actual deceased tuna, preserving the surface features and details of the appendages. The model was instrumented with 32 wall pressure sensors; experiments were performed in a tow tank. Results from flow visualization, drag, and wall pressure measurements over a range of speeds and varying angles of attack are presented.

15. SUBJECT TERMS

Drag Reduction Fluid Dynamics Laminar Flow Propulsion Mechanism Turbulent Boundary Layer

16. SECURITY CLASSIFICATION OF:			17. LIMITATION OF ABSTRACT	18. NUMBER OF PAGES	19a. NAME OF RESPONSIBLE PERSON
a. REPORT (U)	b. ABSTRACT (U)	c. THIS PAGE (U)	SAR	20	Kimberly M. Cipolla
					19b. TELEPHONE NUMBER *(Include area code)* (401) 832-5211

TABLE OF CONTENTS

Section **Page**

LIST OF ILLUSTRATIONS

Figure **Page**

LIST OF TABLES

Table **Page**

LIST OF ABBREVIATIONS AND ACRONYMS

DOF	Degree of Freedom
DPIV	Digital Particle Image Velocimetry
FY	Fiscal Year
HPV	Human-Powered Vehicle
NACA	National Advisory Committee for Aeronautics
NUWC	Naval Undersea Warfare Center
UUV	Unmanned Underwater Vehicle

CHARACTERIZATION OF THE BOUNDARY LAYERS ON FULL-SCALE BLUEFIN TUNA

1. INTRODUCTION

1.1 PURPOSE

The physics that enable tuna to cross large expanses of ocean while feeding and avoiding predators are not yet understood. Research to date suggests that the phenomenon may involve complex control of turbulent boundary layer transition and drag reduction on the body. The typical swimming speed of bluefin tuna is 1 – 2 m/s, but it can be higher during strong accelerations. The goal of the work documented in this report was to experimentally determine the approximate lateral location at which transition to turbulence occurs on the tuna for various speeds. The findings would provide the answer as to whether laminar flow or an advanced propulsion mechanism (or both) allows the bluefin to swim at high speeds. In both scenarios, the technical knowledge gained could be used by the Navy to develop next-generation sonar systems and improve the design of unmanned vehicles. The results could ultimately be applied to the development of advanced naval capabilities for areas as diverse as flow-noise mitigation for towed arrays, torpedo-drag reduction by control surface manipulation, and advancements in bio-inspired propulsion.

1.2 BACKGROUND

The naval hydrodynamics community has extensively studied the delay of transition of the turbulent boundary layer. To date, the majority of the research has focused on rigid vehicles with somewhat simple geometries. For the case of a swimming tuna with multiple degrees of freedom (DOF) and a complex shape, the fluid dynamics problem becomes much more complicated. A logical approach to the problem is to first understand the flowfield around a tuna with a reduced number of DOF. Based on this concept, a full-scale rigid model of a tuna was fabricated and instrumented for tests performed in a tow tank at the Naval Undersea Warfare Center (NUWC) Division Newport, RI. As the project progresses, isolating and understanding the changes in the flowfield due to the presence of gills, manipulating fins, body compliance, and their surface is possible. Determining the effect of each of these features on the abilities of the tuna will provide a framework for future application to Navy systems.

1.3 SCOPE

Much work has been done on the mechanics of fish swimming, mainly focusing on vortex shedding and their mode of propulsion. Many potential flow models for various maneuvers have been developed and studied, but none of these accounts for the detailed behavior of the flow in the boundary layer on which skin-friction reduction and flow-noise mitigation—

two impotant technical challenges to the Navy—are highly dependent. Among researchers in the biomechanics community, there is still debate regarding the ratio of skin friction drag to form drag, and of the comparison of rigid body drag to that of a swimming fish.[1] Also, it has not been definitively established if fish body shapes have evolved primarily to optimize locomotion or if other factors are involved.[2] It is generally accepted that the tuna shape lends itself to minimizing energy consumption; however, from a hydrodynamics view, there may be some mechanism at work in the boundary layer, given the high swimming speeds achieved by the fish.

Hypotheses include changes in the rate of growth of the boundary layer or an effect caused by the presence of a streamwise pressure gradient. Identifying the specific mechanism necessitates detailed experimental measurements of the boundary layer that develops. This type of experiment has not been conducted on a live tuna or a model. From a sensor design perspective, determining if the tuna has developed the capability to sense pressure fields in a high flow-noise environment could lead to a novel, bio-inspired acoustic sensor. Song et al. studied the structure of bluefin tuna ears and found that the material occupying the cavity is much denser than other fish species.[3] The authors hypothesize that this finding indicates an evolutionary adaptation to offer protection during strong accelerations and large depths or to enable hearing during high-speed turns.

Though tuna have been studied in the context of the biology and mechanics of their swimming behavior, from a hydrodynamics perspective, several fundamental questions remain unanswered:

1. Does laminar or turbulent boundary layer separation occur on a tuna? Separation and reattachment of a turbulent boundary layer is typically associated with elevated wall pressure levels and significantly increased drag. Boundary layer separation in complex flowfields is an ongoing area of basic research in the fluid mechanics community.

2. Does transition from a laminar boundary layer to a turbulent boundary layer take place on a tuna at normal swimming speeds? It is expected that the tuna would want to delay transition to minimize drag and reduce heat transfer to the surrounding fluid; however, discontinuities such as the tuna's mouth could generate vorticity and cause local transition to turbulence. The effects of other surface features on the delay and control of transition also have not been quantified. If transition does occur on the body it is important to quantify the variation of this location with speed.

3. Does vortex shedding, which would impact the flow-noise field, occur when a tuna is gliding at an angle of attack? Vortex shedding around a tuna is likely to induce wall pressure fluctuations and negatively impact the tuna's ability to perceive predators and sources of food. A longer term goal of this investigation is to determine if vortex shedding is somehow minimized in regions of the tuna's body that are used to sense pressure fields in the water.

The purpose of this investigation was to answer these questions and subsequently identify Navy systems and research areas that could benefit from the results, such as, torpedo and unmanned underwater vehicle (UUV) drag reduction by control surface manipulation, flow-noise mitigation for towed arrays, and advancements in bio-inspired propulsion.

2. TECHNICAL APPROACH

Simply using arc length Reynolds number and flat-plate equations to predict where transition occurs on a tuna body is an oversimplification. Uncertainties include the surface roughness of the skin, local favorable and adverse pressure gradients, and discontinuities such as the open mouth or juncture at the fins. Historically, much of the fluid mechanics work on fish locomotion has focused on vortex-shedding issues rather than the boundary layer characteristics. This investigation focused on obtaining information on the boundary layer characteristics of a rigid tuna model. In particular, a full-scale model of a Pacific bluefin tuna (see figure 1) was fabricated using a mold made from an actual deceased tuna, preserving the surface features and details of the appendages (see figure 2). The model is 0.84 meter long and is instrumented with 32 wall pressure sensors including a wavenumber filter. The sensors are 2-mm-diameter cylinders mounted on one side of the model so that their sensing face is flush with the fluid-solid interface. The locations of each sensor relative to the nose are indicated in figure 3.

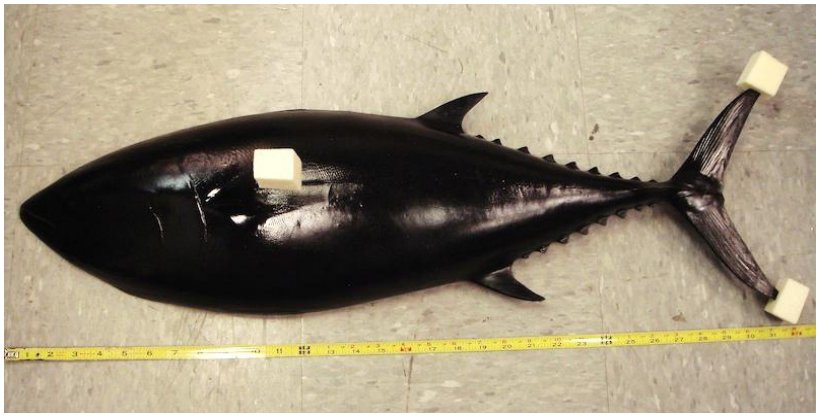

Figure 1. Full-Scale Tuna Model

Figure 2. Details of the Bluefin Tuna Model

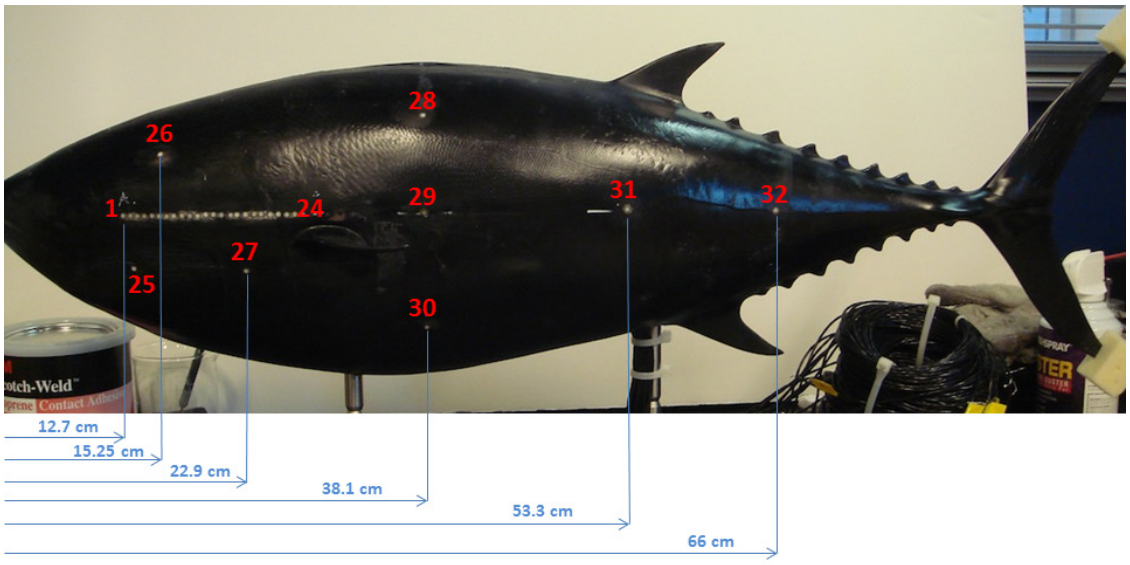

Figure 3. Tuna Model Showing Sensor Locations

Experiments were designed to measure lift, drag, and wall pressure over a range of Reynolds numbers and varying angles of attack using NUWC Division Newport's Code 85 towing tank. The lack of any freestream turbulence intensity makes the tow tank an ideal facility for this experiment. The primary focus of the first year was to determine if transition occurs at speeds up to 3 m/s using flow visualization and wall pressure fluctuation measurements, as well as quantifying lift and drag coefficients as a function of speed. In year two, particle image velocimetry will be used in a larger facility to acquire more details of the flowfield over a wider range of speeds, leading to a better understanding of the nature of the flowfield experienced by the tuna and their ability to swim efficiently at high speeds by minimizing drag.

The majority of the many investigations that have researched the delay of transition in turbulent boundary layers have focused on rigid vehicles with geometric constraints. For the case of a swimming tuna with multiple DOFs and complex shape, the fluid dynamics issue is much more complicated. Using wall pressure sensors as an accurate tool to indicate transition is a well-accepted practice. Purely laminar flow theoretically results in no fluctuations, turbulent spots related to transition result in an intermittent signal, and a fully turbulent boundary layer results in typical random fluctuations. The equally spaced linear array of 24 sensors enables direct measurements of the wavenumber-frequency spectra and allows background acoustic noise to be isolated from the nonacoustic wall pressure fluctuations. In addition, the wall pressure sensors provide a direct measure of the actual flow noise on the tuna for the fully turbulent case.

This investigation used existing instrumentation, data acquisition, and analysis hardware. In addition to the wall pressure sensors, the tow fixture was instrumented with a 6 DOF load cell to measure the total lift and drag on the model. A data acquisition system outfitted with four 16-channel cards collected simultaneous, time-synchronized data from all 32 wall pressure sensors, a reference sensor, and the load cell. A remote control system monitored the acceleration, deceleration, and maximum speed of the tow tank carriage. Sequential runs down the tank were spaced appropriately to allow the water to reach a quiescent state.

3. WORK COMPLETED

In a collaborative effort, Code 15 and Code 85 investigators designed and built a fixture at NUWC Division Newport to interface the model with the carriage in the Code 85 towing tank so the pitch and yaw angles could be adjusted. Fairings were constructed to minimize the drag added by the mounting posts (figure 4). The speed range was 0.5 to 3.0 m/s corresponding to arc-length Reynolds numbers (based on the length of the model) between 4.2×10^5 to 2.5×10^6. Over this range of towing speeds, a transition from laminar to turbulent flow could be expected at some location on the model. Note that vortex shedding related to the surface features and appendages is expected to influence the transition location as well.

Figure 4. Tuna Model Showing Fairings, Angle-Indexing Plate, and Load Cell

Before the start of the experimental measurements, the sensors were connected to the data acquisition system to reveal grounding or electronic noise issues. Connecting the shield on the sensors to the earth ground was found to significantly reduce 60-Hz tones in the signal. Computing the wavenumber-frequency spectra from the 24-sensor linear array also allows the energy from acoustic and nonacoustic sources to be isolated. The focus of these experiments was to measure the nonacoustic energy due to incompressible turbulent wall pressure fluctuations induced by velocity fluctuations within the turbulent boundary layer. Ambient acoustic energy appears as distinct features within the acoustic cone region of the wavenumber-frequency spectrum. The basic array design, including sensor size and spacing, is aimed primarily at resolving the convecting turbulent energy and is similar to linear arrays used in previous investigations.[4, 5, 6]

A grid of small tufts (see figure 5) was attached to the model to facilitate qualitative flow visualization. The tufts are spaced at approximately 2.5 cm and cover the area of the model where the wall pressure sensors are mounted. Two video cameras were attached to the tow

carriage: one mounted underwater just aft of the tow strut (looking forward) and one mounted outside the tank (perpendicular view). Images of the model were captured for the full length of each run as the carriage traveled down the tank. The tow speed was varied from 0.5 to 2.5 m/s depending on the yaw angle, which ranged from 0 to ±18°. The interface between the model and the load cell ensures precise positioning of the model at the desired yaw angle.

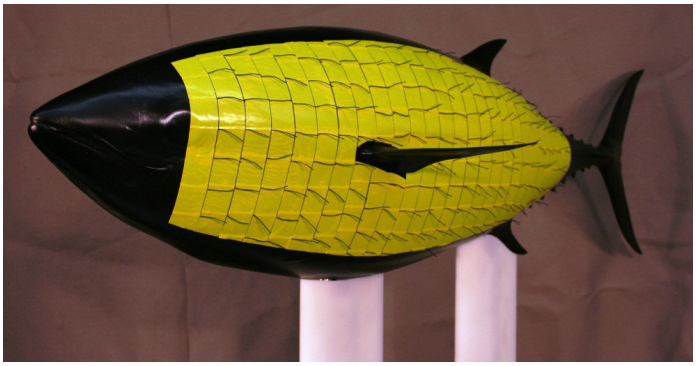

Figure 5. Tuna Model with Tufts Attached

Following completion of the flow visualization experiments, wall pressure data were collected over the relevant range of tow speeds and yaw angles. Spectral analysis (autospectra and wavenumber-frequency spectra) of these data was used to identify regions of laminar, transitional, and turbulent flow. Also, a triaxial accelerometer measured the carriage vibrations to verify that they would have minimal impact on the hydrophone data. The linear array of equally spaced wall pressure sensors allowed a direct measurement of the wavenumber-frequency spectra, $\Phi(\kappa_1,\omega)$ of the turbulent wall pressure fluctuations, where k_1 is the streamwise wavenumber and ω is the radian frequency. Inspection of k-ω spectra will immediately reveal if there is a ridge of convective energy associated with a turbulent boundary layer. In the absence of a convective ridge, the time series from individual wall pressure sensors located further aft can be analyzed to identify regions of turbulent flow downstream of the linear array. Table 1 estimates the approximate transition location (x, measured from the nose) assuming a critical arc length Reynolds number value of 5×10^5. The values are given as the distance in millimeters from the nose of the tuna. At 0.5 m/s and zero yaw angle, a flat-plate boundary layer would be expected to remain laminar over the length of the model. At higher speeds, however, flat-plate estimates would predict transition at some point along the body, occurring near the front of the linear array at the maximum tow speed.

Table 1. Approximate Transition Location Based on Flat-Plate Critical Reynolds Number Value

U_o (m/s)	Critical x (mm)	Nearest Sensor Number
0.5	1000	N/A
1.0	500	31
1.5	333	24, 29
2.0	250	20
2.5	200	12
3.0	167	5

4. RESULTS

The videos obtained during the flow visualization trials were studied to identify features related to laminar, transitional, and turbulent flow. It is evident that, at higher speeds, there is noticeably more turbulence, particularly aft of the pectoral fin. Although the exact localization of turbulent transitions cannot be discerned from the videos alone, some conclusions can be drawn. Figure 6 contains frames from the outboard camera to help illustrate the following points:

1. At zero-degrees yaw and at all speeds (0.5 – 2.5 m/s), the flow appears to be axial and attached along the centerline, forward of the pectoral fin, indicating laminar flow in that region (figure 6a).

2. The flow immediately downstream of the pectoral fin, at most angles and speeds, is separated and reverse flow is evident (figure 6a).

3. At higher angles of attack, for example, 18°, flow on the pressure side displays circumferential components that are symmetric about the centerline (figure 6b).

4. Adding a trip near the eye of the model causes separation and reverse flow immediately downstream at speeds as low as 0.5 m/s (figure 6c); however, the flow quickly reattaches, even at the highest speeds (figure 6d).

Unfortunately, these qualitative results were not sufficient to identify the exact location of turbulent transition or significantly narrow the parameter range of interest.

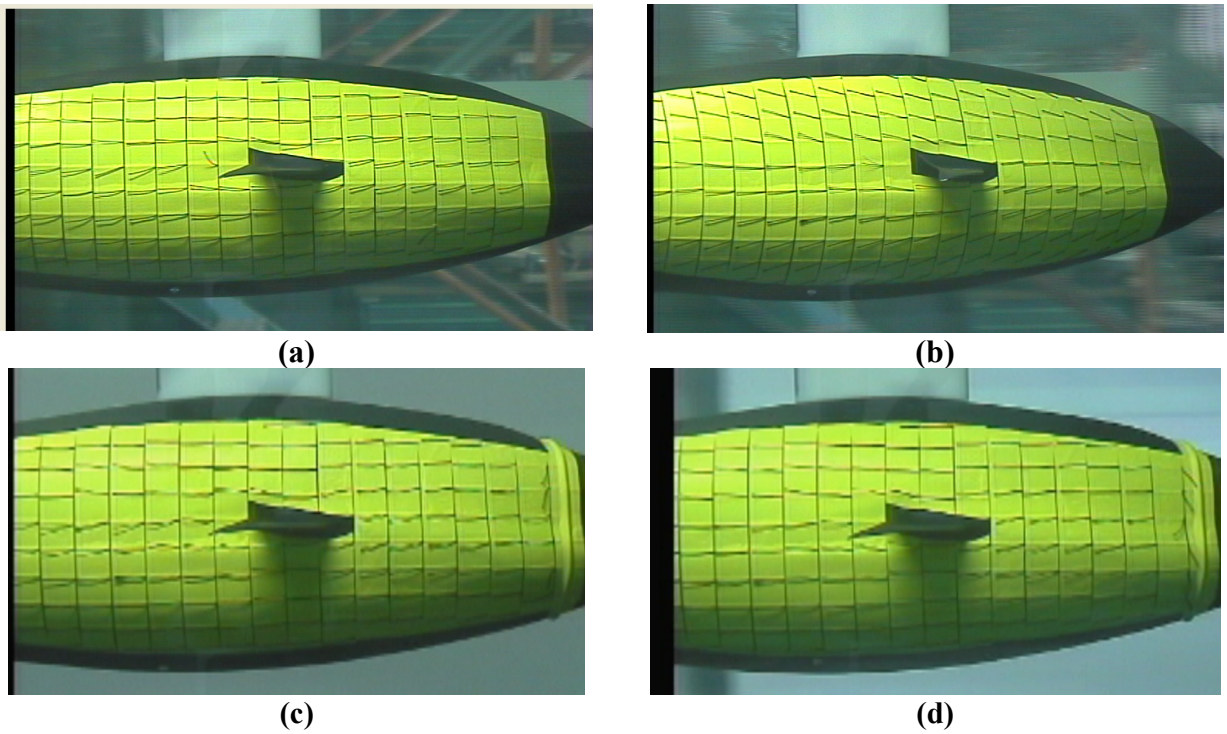

Figure 6. Video Frames Acquired During Flow Visualization Experiments

The mold used to create the model was laser-scanned to generate an electronic copy of the tuna, which facilitated the study of the shape of the body at various cross sections. Inspection of the centerline cross section shown in figure 7a (coincident with the 24 linearly placed wall pressure sensors) reveals a shape that is similar to two-dimensional low-drag airfoils, with a maximum thickness of 127.5 mm (5.02 in.) at 331.5-mm (13.05 in.) chord, or x/c = 45%. The maximum thickness-to-chord ratio (t_{max}/c = 17.2%) and the location of t_{max} are similar to the NACA 66_3-018 shape[7] shown in figure 7b. The point of minimum pressure likely occurs where the thickness of the body begins to taper off at approximately 376 mm (14.8 in.) and is just forward of a distinct change in the surface of the tuna's skin (see figure 8). Cuts at additional vertical locations (figure 9a) show the asymmetry of the tuna body (figure 9b – 9d), which is consistent with the presence of a strong three-dimensional component to the flowfield. This finding will be investigated in fiscal year (FY) 15.

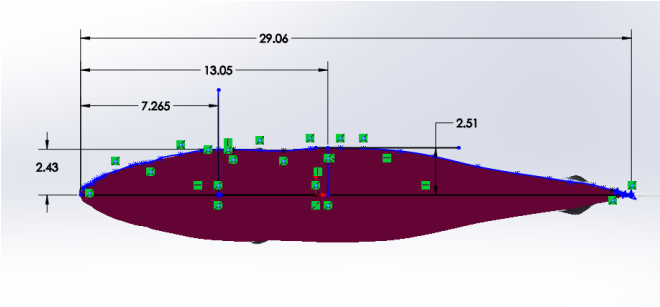

(a)

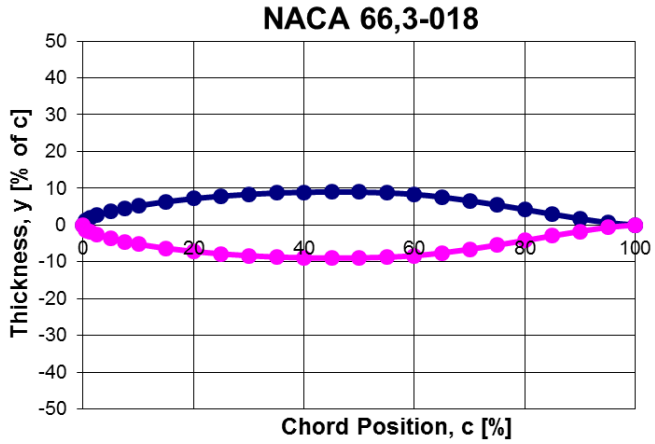

(b)

Figure 7. Comparison of (a) Centerline Cross Section of Tuna Model and (b) NACA Low-Drag Airfoil Shape

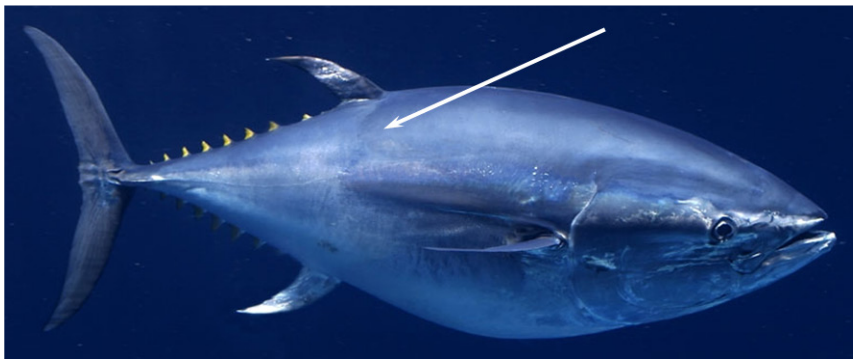

Figure 8. Photo of Pacific Bluefin Tuna Showing Surface Features (Arrow Points to Probable Area of Minimum Pressure)

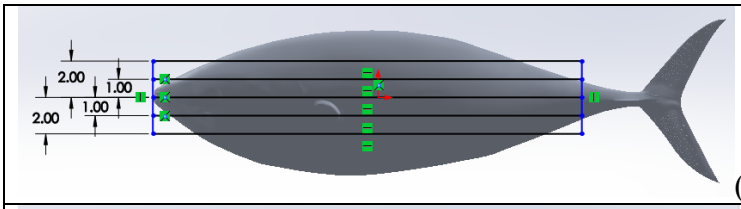

(a) Cuts at additional vertical locations

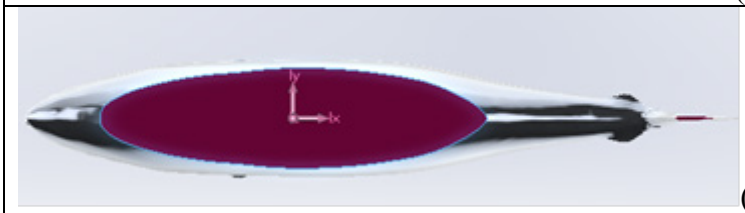

(b) 5 cm above centerline

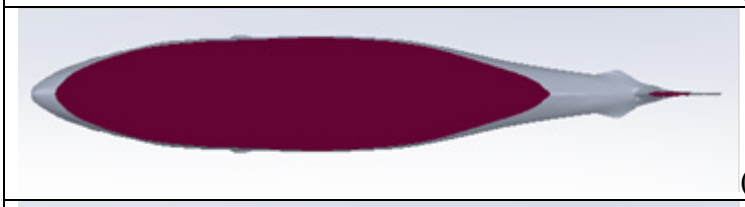

(c) 2.5 cm above centerline

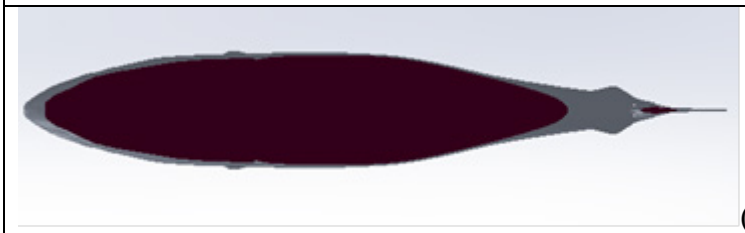

(d) 2.5 cm below centerline

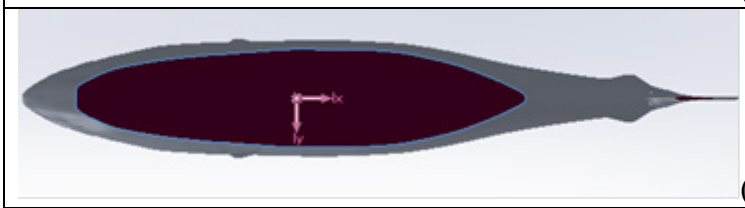

(e) 5 cm below centerline

Figure 9. Cross-Sectional Cuts at Various Vertical Locations

The forces measured with the 6-DOF load cell were used to compute the drag coefficient on the model. Figure 10 illustrates these data with the gross (blue dots) and net (red squares) axial loads plotted as a function of tow speed. The gross values include the loads due to the strut fairings, which were NACA 63_4-021 wing sections with a 101.6-mm (4 in.) chord and a 279.4-mm (11 in.) wetted length. The drag coefficent values C_D are shown as a function of length Reynolds number Re_L in figure 11. The knee in the curve at approximately 1.25×10^6 indicates a shift from a regime of extensive laminar separation aft of the point of minimum pressure to a longer region of attached flow. As the Reynolds number increases above this value, the measured drag coeffient decreases and approaches the value expected for a two-dimensional NACA 66_3-018 airfoil, for example, $C_D = 0.005$ at an $\mathrm{Re}_L = 3 \times 10^6$. At higher values of Re_L (outside the range tested in this experiment), a trend of increasing C_D would be expected because of a sudden forward movement of the point of transition. Follow-on experiments in FY15 will be designed to quantify the upper limit of the low-drag coefficient region.

The wavenumber-frequency spectra for 1 m/s and 3 m/s are shown in figures 12a and 12b, resectively. Note that the 24 sensors that comprise the wall pressure sensor array are located in the favorable pressure region of the body. The time series were highpass-filtered to eliminate the very low frequency contamination from tow carriage vibrations. Although features associated with acoustic noise are apparent, there is no evidence of convecting turbulence even at the highest speed tested. The experiments were repeated with a trip placed near the eye of the tuna model. The resulting wavenumber-frequency spectra at 3 m/s are shown in figure 12c. The trip had the effect of increasing the measured fluctuating wall pressure levels by approximately 20% and producing a convective feature with a wavespeed ≈ 2.5 m/s (highlighted by a dotted line). This wavespeed corresponds to a nondimensional convection velocity $U_c/U_o = 0.83$, which is characteristic of turbulent flow (where U_o is the freestream speed). This spectrum, however, does not display the convective ridge of energy typically associated with a fully developed turbulent boundary layer. For comparison, an example of a spectrum captured with a similar array of sensors in a fully turbulent flow is shown in figure 13.

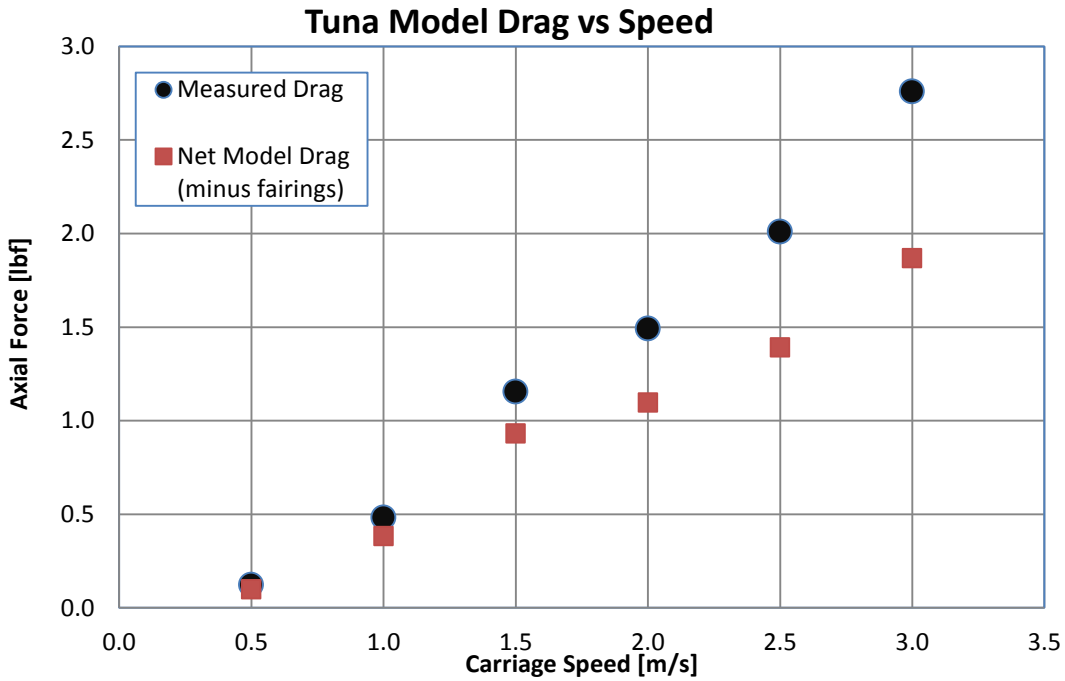

Figure 10. Measured Axial Load on the Tuna Model and Fairings As a Function of Speed

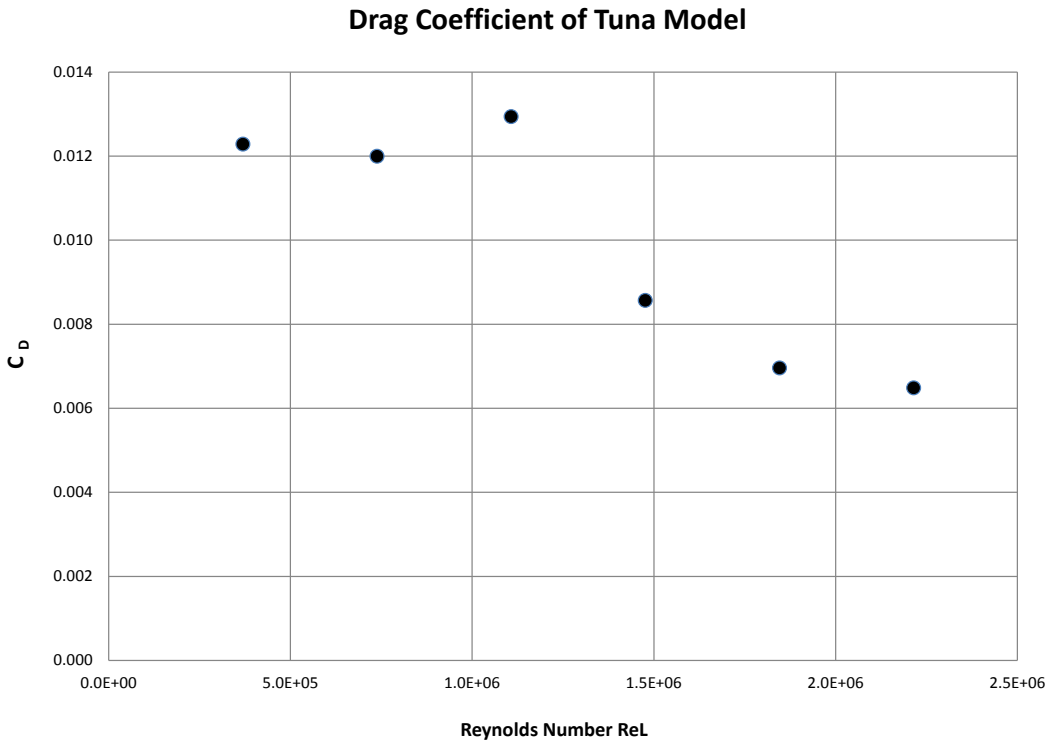

Figure 11. Measured Drag Coefficient on the Tuna Model As a Function of Length Reynolds Number

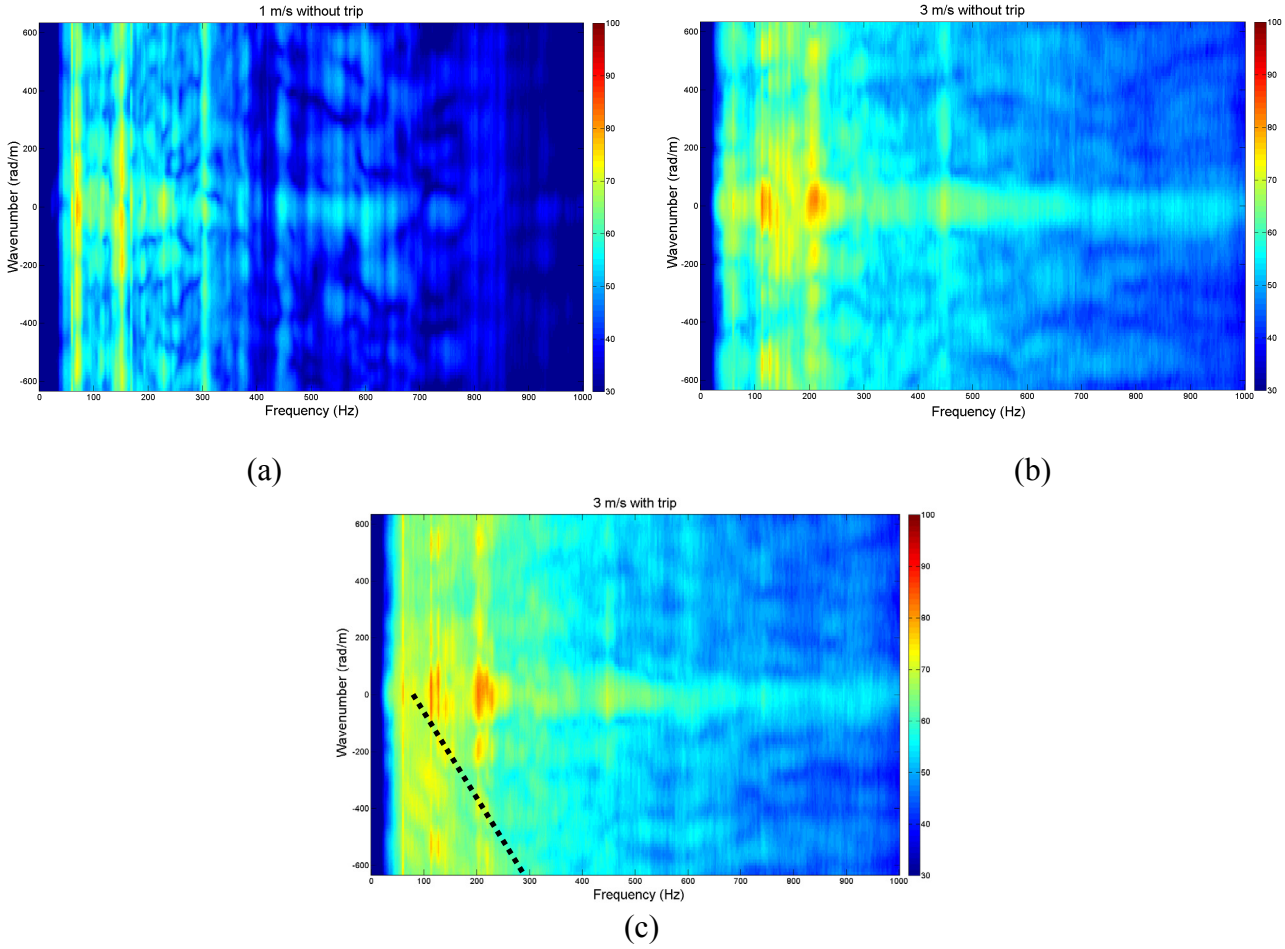

Figure 12. Wavenumber-Frequency Spectra for Select Runs (a) 1 m/sWithout a Boundary Layer Trip, (b) 3 m/s Without a Boundary Layer Trip, and (c) 3 m/s with a Boundary Layer Trip

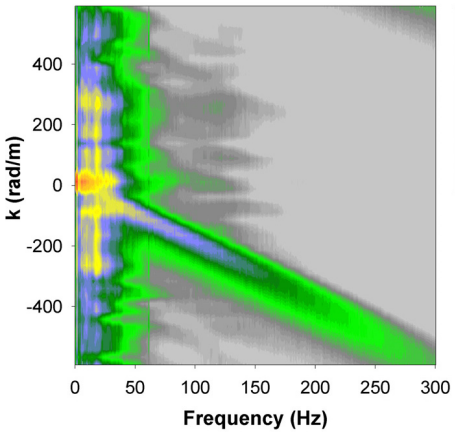

Figure 13. Example of a Wavenumber-Frequency Spectrum Exhibiting a Convective Ridge

5. CONCLUSIONS

The wall pressure data and flow visualization indicate that the flow is not fully turbulent over the range of speeds tested in FY14. The favorable pressure gradient that exists over the front half of body delays the transition from laminar to turbulent flow. For a "laminar" airfoil in this Reynolds number range, transition is expected to occur at the point of minimum pressure, which is estimated to be $x/c = 0.51$ on the tuna body, slightly forward of sensor 31. To obtain more detailed measurements of the flowfield over a larger speed range, a new experiment is being designed for FY15. These measurements will involve digital particle image velocimetry (DPIV) to quantify the mean and fluctuating velocity components and will determine the boundary layer growth over the tuna model. These data will be used to determine the transition location as a function of speed as well as quantify the boundary layer parameters used for scaling and the effects of three-dimensional flow. The primary objectives for FY15 research are to quantify C_D as a function of Re_L and to determine the maximum speed at which the flow remains laminar over a portion of the body.

The results from this project have the potential to influence the designs of next-generation sonar systems and unmanned vehicles. Applications include flow-noise mitigation for towed and hull arrays, reduction of drag and power consumption for torpedoes and UUVs, human-powered vehicles (HPVs), and advances in bio-inspired propulsion.

REFERENCES

1. I. Borazjani and F. Sotiropoulos, "Numerical Investigation of the Hydrodynamics of Carangiform Swimming in the Transitional and Inertial Flow Regimes," *The Journal of Experimental Biology*, vol. 211, pp. 1541-1558, 2008.

2. G. Tokic and D. K. P. Yue, "Optimal Shape and Motion of Undulatory Swimming Organisms," *Proceedings of the Royal Society Biological Sciences*, 2012.

3. J. Song, A. Mathieu, R. F. Soper, and A. Popper, "Structure of the Inner Ear of Bluefin Tuna Thunnus Thynnus," *Journal of Fish Biology*, vol. 68, pp. 1767-1781, 2006.

4. B. M. Abraham and W. L. Keith, "Direct Measurements of Turbulent Boundary Layer Wall Pressure Wavenumber-Frequency Spectra," *ASME Journal of Fluids Engineering*, vol. 120, pp. 29-39, March 1998.

5. W. L. Keith, K. M. Cipolla, and D. Furey, "Turbulent Wall Pressure Fluctuation Measurements on a Towed Model at High Reynolds Numbers," *Experiments in Fluids*, vol. 46, no. 1, pp. 181-189, January 2009.

REFERENCES (Cont'd)

6. K. M. Cipolla and W. L. Keith, "Measurements of the Wall Pressure Spectra on a Full Scale Experimental Towed Array," *Ocean Engineering*, vol. 35, pp. 1052 – 1059, March 2008.

7. I. H. Abbot and A. E. Von Doenhoff, *Theory of Wing Sections*, Dover Publications, Inc., New York, 1959.

INITIAL DISTRIBUTION LIST

Addressee	No. of Copies
Office of Naval Research (ONR 321MS, C.M. Traweek)	1
Defense Technical Information Center	1
Center for Naval Analyses	1
George W. Woodruff School of Mechanical Engineering/Georgia Institute of Technology (D. Trivett)	1
Center for Ocean Engineering/Massachusetts Institute of Technology (A. Techet)	1
Hopkins Marine Technology/Stanford University (B. Block)	1